JOURNAL OF RAMAN SPECTROSCOPY
J. Raman Spectrosc. 2008; **39**: 95–107
Published online 1 October 2007 in Wiley InterScience
(www.interscience.wiley.com) DOI: 10.1002/jrs.1822

JRS

Antioxidant phenolic esters with potential anticancer activity: A Raman spectroscopy study

R. Calheiros,[1] N. F. L. Machado,[1] S. M. Fiuza,[1] A. Gaspar,[1] J. Garrido,[1,2] N. Milhazes,[1,3] F. Borges[1,4] and M. P. M. Marques[1,5]*

[1] Unidade I &D 'Química-Física Molecular', Faculdade de Ciências e Tecnologia, Universidade de Coimbra, 3000 Coimbra, Portugal
[2] Departamento de Engenharia Química, Instituto Superior de Engenharia do Porto, 4200-072 Porto, Portugal
[3] Instituto Superior de Ciências da Saúde, Norte, 4585-116 Gandra, PRD, Portugal
[4] Departamento de Química Orgânica, Faculdade de Farmácia, Universidade do Porto, 4050-047 Porto, Portugal
[5] Departamento de Bioquímica, Faculdade de Ciências e Tecnologia, Universidade de Coimbra, Ap. 3126, 3001-401 Coimbra, Portugal

Received 12 June 2007; Accepted 26 July 2007

A Raman study of hydroxycinnamic and hydroxybenzoic esters (caffeates, ferulates and gallates) displaying antioxidant and anticancer properties was undertaken, with particular emphasis on the analysis of the effect of the ring substituents and the nature of the ester alkyl chain on their spectroscopic features. A complete assignment of the spectra was carried out for all the compounds investigated, in the light of the corresponding calculated wavenumbers (at the density functional theory level). Distinct vibrational patterns were observed for each type of ester, thereby allowing their ready characterisation and identification by Raman spectroscopy. Evidence of the occurrence of intermolecular hydrogen bonds, leading to the formation of dimers in the condensed phase, was also obtained. Copyright © 2007 John Wiley & Sons, Ltd.

Supplementary electronic material for this paper is available in Wiley InterScience at http://www.interscience.wiley.com/jpages//suppmat/

KEYWORDS: Raman spectroscopy; phenolic esters; caffeates; ferulates; gallates; anticancer

INTRODUCTION

Hydroxycinnamic and hydroxybenzoic esters, present in most fruits and vegetables,[1–4] display a huge variety of biological functions[5–11] such as antioxidant capacity, anti-inflammatory action and carcinogenesis modulation.[12–16] However, despite its undisputable importance for human health, the mechanisms underlying the absorption and metabolism of this type of compounds after food consumption are still scarcely known.[17] The evaluation of the antioxidant and antiproliferative activity of this type of phenolic derivatives, either of natural or synthetic origin, as well as the identification of their specific molecular targets, is nowadays an important area of research in the field of medicinal chemistry. In fact, numerous studies have been carried out in order to obtain new lead compounds for the design of cancer preventive or therapeutic agents.[10,18] Nevertheless, even though there is a wealth of data on the relevance of phenolic compounds as growth-inhibiting compounds, the correlation between anti-tumour activity and chemical structure is far from clear.

Caffeic acid (*trans*-3-(3,4-dihydroxyphenyl)-2-propenoic acid, CA) and its ester derivatives have been synthesised recently and screened for their antioxidant and anticancer activities.[9,10,19–24] Methyl caffeate (MC), propyl caffeate (PC) and octyl caffeate (OC) were found to display significant antiproliferative and cytotoxic effects towards human cervix adenocarcinoma (HeLa), coupled to a low toxicity against non-neoplastic cells,[23] which is in accordance with reported data for other hydroxycinnamic synthetic analogues.[25] Ferulic acid (*trans*-3-(4-hydroxy-3-methoxyphenyl)-2-propenoic acid, FA) is the most abundant hydroxycinnamic acid in the plant world and has been described to be an effective antioxidant, essential for preserving the physiological integrity of cells.[26–28] Gallic acid (3,4,5-trihydroxybenzoic acid, GA) and its ester derivatives, in turn, are hydroxybenzoic compounds used as antioxidant additives in both food and pharmaceutical industry – E-310 (propyl gallate) and E-311 (octyl gallate).

The antioxidant and antiproliferative properties of these phenolic derivatives have been proposed to be ruled by specific structure–activity relationships (SARs). The

*Correspondence to: M. P. M. Marques, Departamento de Bioquímica, Faculdade de Ciências e Tecnologia, Universidade de Coimbra, Apartado 3126, 3001-401 Coimbra, Portugal.
E-mail: pmc@ci.uc.pt

biological function of phenolic esters, in particular, is recognised to be strongly dependent on the number and relative orientation of the ring substituents – either hydroxyl or methoxyl – as well as on the presence of an alkyl ester side chain of variable length, chemical nature and spatial orientation (e.g. linear *vs* branched). Moreover, the lipophilicity of these systems (an important measure of their capacity to cross cell membranes) is also closely related to their conformational characteristics, being mainly determined by the number of ring OH's and the type of ester chain.[23] Therefore, a rational design of novel phenolic chemopreventive and/or chemotherapeutic agents demands an accurate and unequivocal structural characterisation of the newly synthesised compounds, in order to accurately predict their *in vivo* pharmacokinetic and pharmacodynamic behaviour.

The present work reports a thorough Raman spectroscopic analysis of a series of structurally related antioxidant phenolic esters (CA, FA and GA derivatives, Fig. 1): methyl *trans*-3-(3,4-dihydroxyphenyl)-2-propenoate (MC), ethyl *trans*-3-(3,4-dihydroxyphenyl)-2-propenoate (ethyl caffeate, EC), propyl *trans*-3-(3,4-dihydroxyphenyl)-2-propenoate (PC), isopropyl *trans*-3-(3,4-dihydroxyphenyl)-2-propenoate (isopropyl caffeate, IPC), butyl *trans*-3-(3,4-dihydroxyphenyl)-2-propenoate (butyl caffeate, BC), octyl *trans*-3-(3,4-dihydroxyphenyl)-2-propenoate (OC), dodecyl *trans*-3-(3,4-dihydroxyphenyl)-2-propenoate (dodecyl caffeate, DC), methyl *trans*-3-(4-hydroxy-3-methoxyphenyl)-2-propenoic acid (methyl ferulate, MF), ethyl *trans*-3-(4-hydroxy-3-methoxyphenyl)-2-propenoic acid (ethyl ferulate, EF), propyl *trans*-3-(4-hydroxy-3-methoxyphenyl)-2-propenoic acid (propyl ferulate, PF), methyl 3,4,5-trihydroxybenzoate (methyl gallate, MG), ethyl 3,4,5-trihydroxybenzoate (ethyl gallate, EG), propyl 3,4,5-trihydroxybenzoate (propyl gallate, PG), isopropyl-3,4,5-trihydroxybenzoate (isopropyl gallate, IPG), butyl 3,4,5-trihydroxybenzoate (butyl gallate, BG), octyl 3,4,5-trihydroxybenzoate (octyl gallate, OG) and dodecyl 3,4,5-trihydroxybenzoate (dodecyl gallate,DG). The results obtained were interpreted in the light of the conformational data yielded by quantum mechanical calculations presently carried out for the ferulates and gallates (at the density functional theory level), and previously applied to the caffeates and some of their analogues.[18,29–31]

EXPERIMENTAL

Reagents

Dimethylsulfoxide (spectroscopic grade), *trans*-CA, *trans*-FA, GA, MG, EG, PG, BG, OG and DG were purchased from Sigma-Aldrich Química S.A. (Sintra, Portugal). Dimethylsulfoxide-d_6 (99.8%) and all other reagents and solvents (*pro analysis* grade) were obtained from Merck (Lisbon, Portugal).

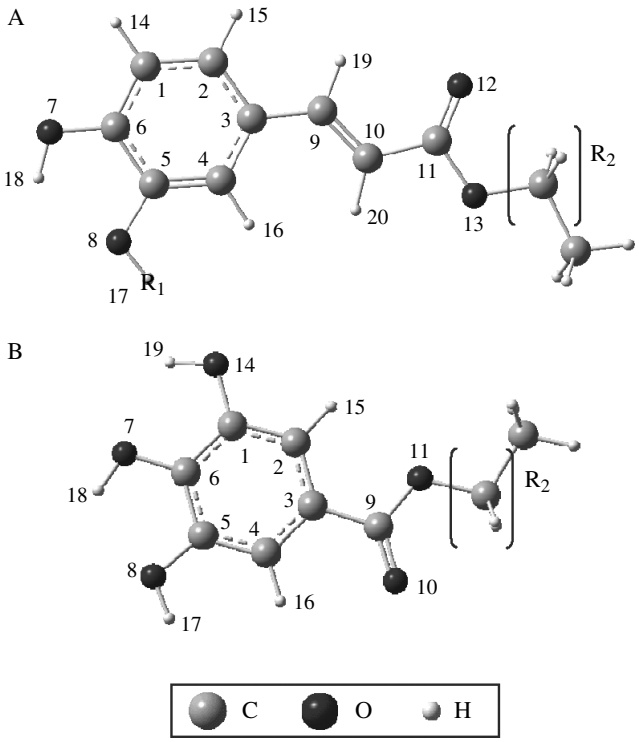

Figure 1. Schematic representation of the most stable calculated conformers for the hydroxycinnamic (A) and trihydroxyphenyl (B) esters studied in the present work. A – R_1 = H – caffeates; R_1 = CH_3 – ferulates; B – gallates; R_2 = $(CH_2)_n$, n = 0, 1, 2, 3, 7, 11 for methyl, ethyl, propyl, butyl, octyl and dodecyl esters, respectively; R_2 = $(CHCH_3)$ for isopropyl esters. (The atom numbering is included, with the exception of the alkyl ester group. The structure depicted in A refers to a *S-cis/anti* conformation, while the one in B represents a *S-cis/syn* conformation).

Synthesis

Apparatus

Infrared spectra were recorded on an ATI Mattson Genesis Series FTIR spectrophotometer using potassium bromide disks. Only the most significant absorption bands are reported ($\upsilon_{max.}$ in cm^{-1}). ^1H and ^{13}C NMR data were acquired (at room temperature) on a Bruker AMX 300 spectrometer, operating at 300.13 and 75.47 MHz, respectively. Dimethylsulfoxide-d_6 was used as the solvent; chemical shifts are expressed in δ (ppm) values relative to tetramethylsilane (TMS) as internal reference; coupling constants (J) are given in Hz. Assignments were also made from distortionless enhancement by polarization transfer (DEPT) experiments ((underlined values). Electron impact mass spectra (EI-MS) were carried out on a VG AutoSpec instrument, the data being reported as m/z (% of relative intensity of the most important fragments). Melting points were obtained on a Köfler microscope (Reichert Thermovar) and are uncorrected.

DOI: 10.1002/jrs

Other conditions

Thin-layer chromatography (TLC) was performed on pre-coated silica gel 60 F254 (E. Merck) with a layer thickness of 0.2 mm. The following systems were used for analytical control: silica gel, diethyl ether; silica gel, chloroform/methanol (9 : 1). The spots were visualised under UV light (254 and 366 nm) and iodine vapour. Solvents were evaporated in a Buchi Rotavapor.

General synthetic procedure

The methyl-, ethyl-, propyl-, isopropyl- and butyl- esters of caffeic and ferulic acids as well as IPG were synthesised by acid catalysis Fischer esterification following the procedure developed by Borges and co-workers.[23,30] The alkyl esters were characterised by NMR and MS; for some esters, the data is in accordance with previously reported results.[21,23,30,32,33]

Octyl caffeate (octyl *trans*-3-(3,4-dihydroxy-phenyl)-2-propenoate, OC) and dodecyl caffeate (dodecyl *trans*-3-(3,4-dihydroxyphenyl)-2-propenoate, DC) were obtained *via* a nucleophilic substitution reaction, that takes place between the corresponding alkyl halides and sodium caffeate, using dimethylformamide as solvent.[6]

BC – Yield 90%; IR: 3484 (OH), 3339 (OH), 2951, 2865, 1682 (C═O), 1637, 1600, 1533, 1441, 1364, 1274, 1181, 1101, 971, 849, 810, 529. ^{1}H NMR δ: 0.90 (3H, t, $COO(CH_2)_3$ $C\underline{H}_3$), 1.36 (2H, *m*, $COO(CH_2)_2C\underline{H}_2CH_3$), 1.60 (2H, m, $COOCH_2C\underline{H}_2CH_2CH_3$), 4.10 (2H, m, $COOC\underline{H}_2(CH_2)_2CH_3$), 6.27 (1H, d, J = 15.9, H(α)), 6.77 (1H, d, J = 8.1 (H5)), 6.99 (1H, m, (H6)), 7.05 (1H, d, J = 2.0 (H2)), 7.46 (1H, *d*, J = 15.9, H(β)). ^{13}C NMR δ: 23.3 [$O(CH_2)_3\underline{C}H_3$], 28.4 ($OCH_2CH_2\underline{C}H_2CH_3$), 40.0 ($OCH_2\underline{C}H_2CH_2CH_3$), 73.2 ($O\underline{C}H_2CH_2CH_2CH_3$), 123.8 (CHAr), 124.3 (CHAr), 125.5 (CHAr) 131.2(C(α), 135.2 (C-1), 154.7 (CH(β)), 155.3(C–OH), 158.1(C–OH), 176.5 (C═O); EI-MS *m*/*z* (%): 236 ($M^{+\bullet}$, 100); mp 112–114 °C (ethyl ether/*n*-hexane).

IPC – Yield 75%; IR: 3463 (OH), 3309 (OH), 2975, 2929, 1679 (C═O), 1632, 1599, 1530, 1442, 1370, 1274, 1185, 1096, 978, 903, 850, 813, 782, 711, 562. ^{1}H NMR δ: 1.21, 1.24 (6H, s, $COOCH(C\underline{H}_3)_2$), 4.98 (1H, m, $COOC\underline{H}(CH_3)_2$), 6.22 (1H, *d*, J = 15.9 C$\underline{H}$(α)), 6.75 (1H, d, J = 8.1(H5)); 6.98 (1H, d, J = 1.8 (H2)); 7.02 (1H, dd, J = 7.2; 2.1(H6)); 7.44 (1H, d, C*H*(β), J = 15.9); ^{13}C NMR δ: 21.8 ($OCH(\underline{C}H_3)_2$), 66.9 ($OCH(\underline{C}H_3)_2$), 114.4, 114.8,, 115.7 (CH(2, 5, 6)), 121.3 (C(1)), 125.5(CH(α), 144.9 (C–OH), 145.6 (CH(β)), 148.4(C–OH), 166.1 (C═O); EI-MS *m*/*z* (%): 222 ($M^{+\bullet}$, 100); mp 143–147 °C.

MF – Yield 80%; IR: 3394 (OH), 2944 (OH), 1702 (C═O), 1679, 1636, 1596, 1515, 1433, 1265, 1159, 1121, 1027, 979. ^{1}H NMR δ: 3.69 (3H, s, OCH_3), 3.81 (3H, *s*, OCH_3), 6.48 (1H, d, J = 15.9, H(α)), 6.79 (1H, d, J = 8.1 (H5)), 7.12 (1H, dd, J = 8.2; 1.9 (H6)), 7.32 (1H, d, J = 1.9 (H2)), 7.56 (1H, d, J = 15.9, H(β)), 9.62 (1H, s, 4-OH). ^{13}C NMR δ: 51.2 (OCH_3), 55.7 (OCH_3), 111.3 (CHAr), 114.2(C(α), 115.5 (CHAr), 123.1 (CHAr), 125.5 (C-1), 145.1(C-OH), 147.9 (CH(β)), 149.4 (C–O), 167.1 (C═O); EI-MS *m*/*z* (%): 208 ($M^{+\bullet}$, 100); mp 57–60 °C (ethyl eter/*n*-hexane).

IG – Yield 80%; IR: 3498 (OH), 3269 (OH), 1673 (C═O), 1615, 1538, 1463, 1391, 1366,1324, 1224, 1181, 1111, 1025, 976, 865, 745, 629, 502. ^{1}H NMR δ: 1.24, 1.26 (6H, s, $COOCH(C\underline{H}_3)_2$), 5.02 (1H, m, $COOC\underline{H}(CH_3)_2$), 6.93 (2H, s, H2,H6), 8.95 (1H, s, 4-OH), 9.35 (2H, s, 3,5-OH); ^{13}C NMR δ: 21.5 ($OCH(\underline{C}H_3)_2$), 67.0 ($OCH(\underline{C}H_3)_2$), 108.2, CH(2, 6)), 119.7 (CH(1)), 138.0 (C–OH), 145.2(2 × C–OH), 165.1 (C═O); EI-MS *m*/*z* (%): 212($M^{+\bullet}$, 100); mp 126–128 °C.

Raman spectroscopy

The Raman spectra were obtained at room temperature, in a triple monochromator Jobin-Yvon T64000 Raman system (focal distance 0.640 m, aperture *f*/7.5) equipped with holographic gratings of 1800 grooves.mm^{-1}. The pre-monochromator stage was used in the subtractive mode. The detection system was a liquid-nitrogen-cooled, non-intensified 1024 × 256 pixel (1″) charge-coupled device (CCD) chip, and the entrance slit was set to 200 μm.

The 514.5 nm line of an argon ion laser (Coherent, model Innova 300–05) was used as the excitation radiation, providing between 20 and 90 mW at the sample position. A 90° geometry between the incident radiation and the collecting system was employed. The entrance slit was set to 200 μm and the slit between the pre-monochromator and the spectrograph was kept at 12 mm. Samples were sealed in Kimax glass capillary tubes of 0.8 mm inner diameter. Under the above conditions, the error in wavenumbers was estimated to be within 1 cm^{-1}.

Some of the spectra were recorded in a Spex Ramalog 1403 double spectrometer (focal distance 0.85 m, aperture *f*/7.8), equipped with holographic gratings of 1800 grooves.mm^{-1} and a detector assembly containing a thermoelectrically cooled Hamamatsu R928 photomultiplier tube. Slits of 320 μm and a scan speed of 1 cm^{-1}s^{-1} were used.

In order to avoid fluorescence, the spectra of solid CA and GA were recorded in an RFS 100/S Bruker Fourier-transform Raman spectrometer, with a 180° geometry, equipped with an InGaAs detector. Near-infrared excitation was provided by the 1064 nm line of a Nd : YAG laser (Coherent, model Compass-1064/500N). A laser power of 200 mW at the sample position was used, and resolution was set to 2 cm^{-1}.

Quantum mechanical calculations

The quantum mechanical calculations were performed using the GAUSSIAN 03W program,[34] within the density functional theory (DFT) approach in order to properly account for the electron correlation effects (particularly important in this type of conjugated systems). The widely employed hybrid method B3LYP, which includes a mixture of HF and DFT exchange terms and the gradient-corrected correlation functional of Lee, Yang and Parr,[35,36] as proposed and parametrised by Becke,[37,38] was used, along with the double-zeta split valence basis set 6-31G**.[39]

Molecular geometries were fully optimised by the Berny algorithm, using redundant internal coordinates:[40] the bond

DOI: 10.1002/jrs

lengths to within *ca* 0.1 pm and the bond angles to within *ca* 0.1°. The final root mean square (rms) gradients were always less than 3×10^{-4} hartree.bohr^{-1} or hartree.radian^{-1}. No geometrical constraints were imposed on the molecules under study.

Calculation of the vibrational spectra was based on a full geometry optimisation of the phenolic esters. The harmonic vibrational wavenumbers, as well as their Raman activities and infrared intensities, were obtained at the same level of theory. Wavenumbers above 450 cm^{-1} were scaled by 0.9614[41] before comparing them with the experimental data, in order to correct for the anharmonicity of the normal modes of vibration.

RESULTS AND DISCUSSION

Figures 2 and 3 represent the experimental solid-state Raman pattern at room temperature of the series of esters under study (in the 125–1800 cm^{-1} and 2700–3600 cm^{-1} regions respectively) – hydroxycinnamates (caffeates, ferulates) and hydroxybenzoates (gallates). These spectra were interpreted in the light of quantum mechanical data – both previously published results for the caffeates and their analogues[29–31] and theoretical results presently obtained for some of the ferulates and gallates by DFT molecular orbital methods.

As previously reported,[18,23,29–31] the most stable structures for this type of phenolic esters (Fig. 1), which result from a balance between inductive and mesomeric effects, correspond to planar geometries displaying an identical orientation of the aromatic substituents (both OH and OCH_3), a zig-zag conformation of the variable-length ester alkyl chain and an *S-cis* conformation of the carbonyl group (in agreement with published studies on similar molecules).[42,43] Regarding the relative orientation of the ring substituents and the C═O group, it is worth noticing that while an *anti* conformation had been found to be preferred for the caffeates (dihydroxylated)[31] (as for CA[29]), according to the DFT calculations presently carried out a *syn* conformation is favoured for the gallates (trihydroxylated), as previously verified for GA[23] and 3,4,5-trihydroxycinnamates.[18] For the ferulates (monohydroxylated), in turn, the two conformations, *anti* and *syn*, are energetically very close (population difference around 3–5%, at room temperature). In addition, for the hydroxycinnamates an *E*-configuration of the aromatic ring and the C═O group relative to the C_9═C_{10} bond is energetically favoured, as verified for the homologous caffeates.[31]

The Raman features presently observed reflect these geometrical preferences, comprising distinctive features which allow a ready differentiation of the type of ester, namely: (1) cinnamates *vs* benzoates (caffeates and ferulates *vs* gallates), (2) disubstituted *vs* trisubstituted (caffeates and ferulates *vs* gallates), (3) dihydroxylated *vs* monohydroxylated (caffeates *vs* ferulates), (4) methoxy-substituted *vs* hydroxy-substituted (ferulates *vs* caffeates and gallates). Also, each element within these series of esters showed to be distinguishable by its Raman spectrum: even- *versus* odd-membered, and short *versus* long alkyl chain. Tables S1, S2 (Supplementary Material) and 1 contain the experimental Raman wavenumbers for some of the esters presently studied and their acid precursors (the assigned experimental wavenumbers for the other esters are available from the authors upon request).

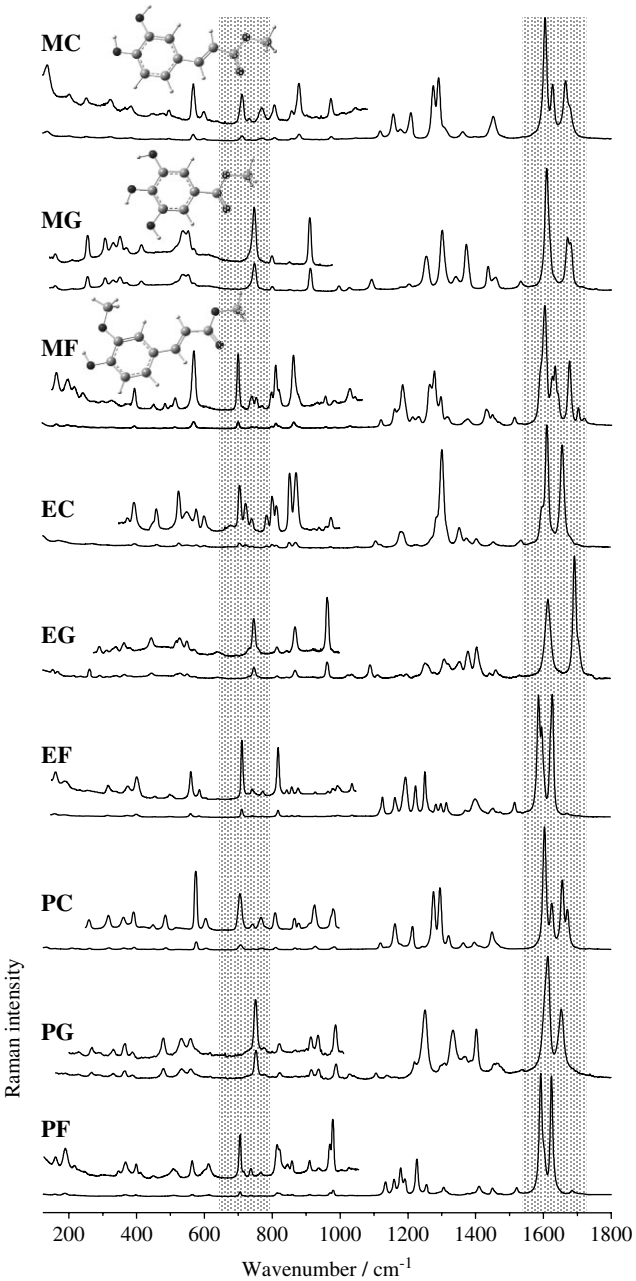

Figure 2. Experimental Raman spectra in the 125–1800 cm^{-1} region of the phenolic esters studied in the present work (solid state, 25 °C).

DOI: 10.1002/jrs

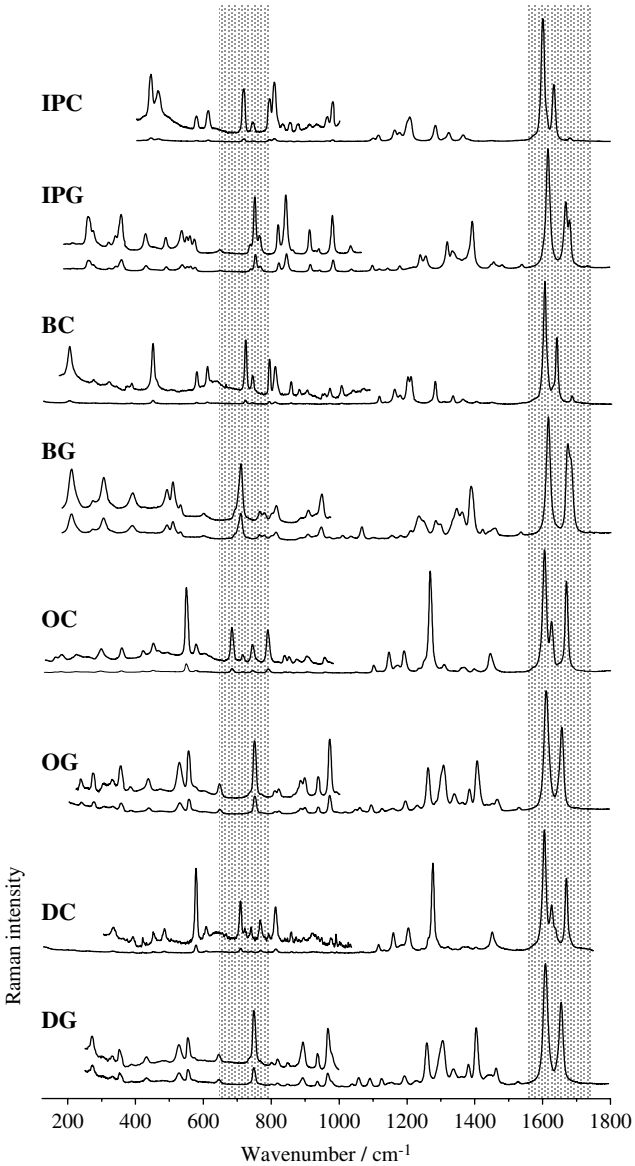

Figure 2. (*Continued*)).

The main Raman bands detected for the phenolic esters under study may be grouped as follows: (Tables S1, S2 and 1, Figs 2 and 3):

1. OH vibrations – stretching modes between 3550 and 3400 cm^{-1} and deformations (bendings) from *ca* 1450–1100 cm^{-1};
2. C═O stretching mode, from 1740 to 1640 cm^{-1};
3. C═C stretching vibrations from the aromatic ring, yielding the most intense bands in the spectrum, between *ca* 1650–1600 cm^{-1}. Despite the very low Raman activity of one of the three $\nu_{C=C}$ features theoretically assigned to these ring modes, it was detected for most of the systems presently studied. In the caffeates and ferulates the unsaturated linker between the ring and the alkyl ester moiety (Fig. 1) gives rise to an extra C═C stretching band, at slightly higher wavenumbers and with a lower Raman activity than the two more intense aromatic $\nu_{C=C}$;
4. CH vibrations – stretching modes, both symmetric and asymmetric, from *ca* 3100 to 2850 cm^{-1}, respectively; and CH_2/CH_3 deformations (scissoring, wagging, twisting and rocking), between *ca* 1450 and 900 cm^{-1};
5. $C–O_{ester}$ stretching vibration – at *ca* 1180 cm^{-1};

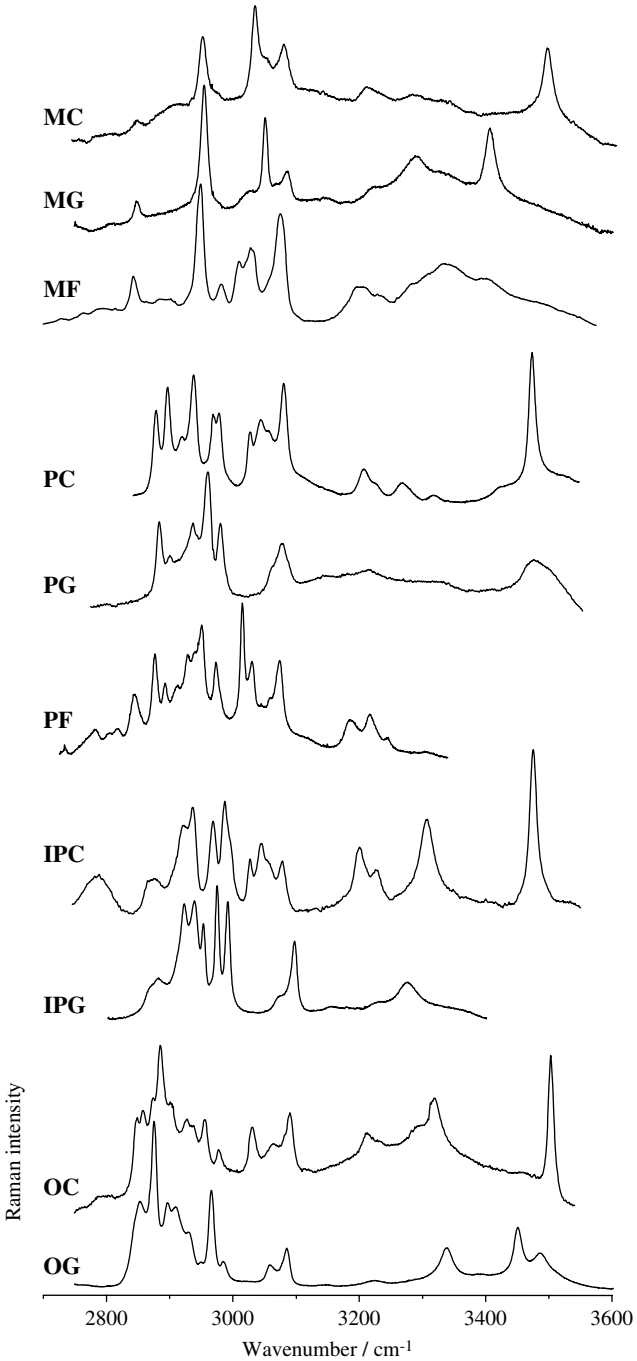

Figure 3. Experimental Raman spectra in the 2700–3600 cm^{-1} region for some of the phenolic esters studied in the present work (solid state, 25 °C).

DOI: 10.1002/jrs

6. $(CH_3)_{ester}$ modes – deformations at *ca* 1450–1400 cm^{-1}, and torsion around 250 cm^{-1} (with a very low Raman activity);
7. $(OCH_3)_{ring}$ vibrations (for the ferulates)–CH_3 stretching modes (both symmetric and asymmetric), from *ca* 3040 to 2900 cm^{-1}, respectively; CH_3 deformations (both symmetric and asymmetric), between *ca* 1460 and 1130 cm^{-1}; the characteristic O–CH_3 stretching mode at *ca* 1025 cm^{-1} (with a very low Raman activity); and the CH_3 torsion, not detected experimentally and theoretically predicted at a higher frequency (200–270 cm^{-1}) – than for the ester methyl groups;
8. For all the esters investigated, a quite intense and well-defined band appears at *ca.* 710–750 cm^{-1}, predicted as a weak signal due to in-plane chain deformation modes (Δ_{C-O-C}) of the ester moiety (Fig. 2 *vs* Figs S1 and S2 (Supplementary Material)).

The spectral data presently gathered clearly evidence the unquestionable fact that these phenolic esters are easily distinguishable by Raman spectroscopy. Some spectral features are particularly useful for achieving this goal:

1. The ferulates have distinct vibrational modes due to the OCH_3 ring substituent –CH_3 stretching modes (3040–2900 cm^{-1}), CH_3 deformations below 1480 cm^{-1} and the characteristic O–CH_3 stretching vibration (*ca* 1180 cm^{-1}) (Figs 2 and 3). Also, the spectral envelope comprising the CH deformations is narrower for these methoxy-substituted esters and appears at lower wavenumbers relative to the homologous caffeates and gallates (1300–1100 cm^{-1} *vs* 1450–1150 cm^{-1}, respectively).
2. The gallates display a less complex spectral pattern in the 1700–1550 cm^{-1} range as compared to the caffeates and ferulates, owing to the absence of the $\nu_{C=C(chain)}$ signal (Fig. 5(C)). Moreover, the corresponding $\nu_{C=O}$ vibration gives rise to a more intense band than the homologous caffeates and ferulates, for which this is usually a moderate to weak feature, sometimes overruled by the strong C=C stretching modes (Fig. 5(A) and (B)).
3. As to the ring OH stretching modes, while for most of the caffeates (MC, PC, IPC, OC, Fig. 3) yield quite intense and definite bands between 3550 and 3400 cm^{-1} (Fig. S2, Tables S1 and S2 (Supplementary Material)), they give raise to much broader features for the gallates, between 3500 and 3200 cm^{-1} (Fig. 3, Table 1). In fact, for these trihydroxylated compounds intramolecular (O)H···O(H)

Table 1. Experimental (solid state) Raman wavenumbers (cm^{-1}) for GA, MG, EG, IPG and PG

Wavenumbers (cm^{-1})					
GA[b]	MG	IPG	PG	DG	[a]Approximate description
3496	3406	3275	3475	3488	ν (O^8H)
3370	3326	3228	3409	3450	ν (O^7H)
3281	3292	3154	3329	3340	ν ($O^{14}H$)
3234					ν ($O^{11}H$)
	3224		3215	3223	$2 \times \phi$ 8a
			3178		(1537 + 1653 cm^{-1})
	3147				(1610 + 1534 cm^{-1})
			3146		(1613 + 1537 cm^{-1})
				3147	(1611 + 1530 cm^{-1})
3102	3087	3096	3078	3085	ϕ 20a
3069	3054	3072	3063	3060	ϕ 20b
	3026	2991	2980	2985	ν_{as} (CH_3) + ν_{as} (CH_2)$^{\Psi}$
		2974			ν_{as} (CH_3)
	2955		2960	2966	ν_s (CH_3) + ν_s (CH_2)
		2952			ν ($C^{12}H$)
			2943	2930	ν_s (CH_2)
		2937			ν_s (CH_3)
		2922	2937		ν_s (CH_3)
				2912	ν_{as} (CH_3) + ν_{as} (CH_2)
			2900		(1251 + 1653 cm^{-1})
				2895	ν_s (CH_2)
			2884		(1219 + 1669 cm^{-1})
		2880			(1393 + 1481 cm^{-1})
				2874	ν_s (CH_2)

(*continued overleaf*)

DOI: 10.1002/jrs

Table 1. (*Continued*)

Wavenumbers (cm^{-1})					
GA[b]	MG	IPG	PG	DG	[a]Approximate description
		2872			$(1255 + 1617\ cm^{-1})$
				2854	$\nu_s\ (CH_2)$
	2850				$(1256 + 1609\ cm^{-1})$
				2728	$(1060 + 1658\ cm^{-1})$
				2694	$(1093 + 1611\ cm^{-1})$
1742	1755	1734			ν (C═O)
1695	1680	1681		1703	ν (C═O)
	1671	1669	1653	1658	ν (C═O)
1616					ϕ 8b + δ ($O^7H + O^8H$)
	1610	1617	1613	1611	ϕ 8b + 8a + δ (OH)
1598			1607		ϕ 8a + δ ($O^7H + O^{14}H$)
1532	1534	1540	1537	1530	ϕ 19a + δ ($O^7H + O^8H$)
1485					ϕ 19b
		1481			$\delta_{as}\ (CH_3)$
	1460	1457		1465	$\delta_{as}\ (CH_3)$
	1437	1449			$\delta_{as}\ (CH_3)$
				1407	sciss. (CH_2)
			1402		$\delta_s\ (CH_3) + \omega\ (CH_2)$
					$\delta_s\ (CH_3) + \delta\ (C^{12}H) + \phi$ 14
1386					ϕ 2 + δ (OH)
1367	1373	1393	1386	1384	δ (OH) + $\delta_s\ (CH_3)$
			1368		ϕ 14 + δ (O^7H)
				1365	$\omega\ (CH_2) + \delta\ (O^{14}H)$
1333					δ ($O^7H + O^{14}H + O^{11}H$) + δ ($C^{12}H$)
	1343		1333	1340	$\phi\ 2^{\xi,\Psi} + \omega\ (CH_2) + \delta\ (O^{14}H)$
		1340			$\delta_s\ (CH_3) + \delta\ (O^{14}H) + \delta\ (CH^{20})$
		1334			$\delta\ (C^{12}H) + \delta_s\ (CH_3)$
1324					δ (OH) + δ (C^4H)
			1309	1308	δ (OH) + $\omega\ (CH_2)^{\Psi}$
1267	1302	1319			ϕ 14 + δ (OH)
	1256				$\nu(CO^7) + \delta$ (OH)
		1255			δ (OH) + δ ($C^{12}H$)
			1251	1261	t $(CH_2) + \phi$ 13 + $\omega\ (CH_2) + \nu\ (CO^{11}) + \nu\ (CC)_{ester}$
		1239			$\delta\ (C^{12}H) + \nu\ (CO^{11}) + \nu\ (CC)_{ester} + \delta$ (OH)
1221			1219	1230	ϕ 18b + δ ($O^7H + O^{14}H$)
				1195	$\omega\ (CH_2)$
	1180			1175	$\delta\ (O^{14}H) + \delta\ (C^2H)$ + r $(CH_3)^{\S}$
		1178			r (CH_3)
				1157	r (CH_2)
			1143		r (CH_2) + r (CH_3)
		1143		1127	δ ($O^7H + O^8H$) + δ (C^4H)
		1119			$\gamma\ (C^{12}H)$
			1106		r $(CH_3) + \nu\ (C^{12}C)$
1103					δ ($O^{11}H$) + δ (C^2H)
	1096			1093	r (CH_3)
1039	1031	1097	1041		ϕ 18a + $\nu\ (O^{11}C)^{\S}$
				1060	$\omega\ (CH_2)$
				1040	$\omega\ (CH_2)$

(*continued overleaf*)

Table 1. (*Continued*)

Wavenumbers (cm^{-1})					
GA[b]	MG	IPG	PG	DG	[a]Approximate description
966		1035	1029	1010	ϕ 7b + ω (CH_2) + δ (O^7H)*
	1000				ϕ 7a + ϕ 1 + ν ($O^{11}C$)
		981	988	968	ϕ 7a + ϕ 1 + ν ($O^{11}C$) + ν $(CC)_{ester}$ + r $(CH_3)^{\Psi}$
877	917		937	938	ϕ 7a + ϕ 1 + ν (C^9O) + ν ($O^{11}C$)* + r $(CH_3)^{\Psi}$
		941			r (CH_3)
		915	914	895	r (CH_3) + ν $(CC)_{ester}{}^{\Psi}$
		864			r (CH_3) + ν ($O^{11}C$)
850	857	843	882	850	γ (C^2H)
807	805			819	γ (C^4H)
		820			r (CH_3) + δ ($C^{12}H$)
			778	802	ϕ 7a + ϕ 1 + Δ (OCO)
		766			r (CH_3)
		751			ϕ 7a + ϕ 1
775	753	738	752	750	ϕ 1
742					ϕ 11 + γ $(OH)_{carbox}$
				734	r (CH_2) + r (CH_3)
		648		646	ϕ 5
574	576	572		576	Δ ($C^2C^3C^9$)
559	558	559	560	555	ϕ 16a + γ $(OH)_{carbox}{}^{**}$
		549			ϕ 16b
548	542	534	533	528	ϕ 6b
454	527	487	488	472	ϕ 6a + 6b
441	421	427		433	γ ($O^7H + O^{14}H)_{op}$
391			388	389	Δ (COC) + Δ (CCC)
360	377			354	γ ($O^7H + O^{14}H)_{ip}$
			366		Δ (COC) + Δ (CCC) + γ ($O^7H + O^{14}H)_{ip}$
	359				Γ ($C^2C^3C^9$) + γ (OH)
		355			Γ $(CCC)_{ester}$ + Δ ($C^3C^9O^{11}$)
		338			γ (OH)
				333	Δ $(CCC)_{ester}$
348	338				ϕ 6a
319		318			Δ ($C^6C^5O^8$) + Δ ($C^2C^1O^{14}$)
	315		331		Δ (COC) + δ $(CO\text{-}CH_3)^{\dagger}$
			290		skeletal modes
273					Δ ($C^1C^6O^7$) + Δ ($C^2C^1O^{14}$)
		272			τ (CH_3)
262	263	257	268	273	ϕ 10a
243	217		228		γ ($O^7H + O^8H)_{ip}$
206	168				skeletal modes
114	134	141			skeletal modes
	112	129			τ (CH_3)
		108			τ (CH_3)

[a] Atoms are numbered according to Fig. 1(b). [b] FT-Raman. The Wilson notation was used for the description of benzene derivatives normal vibrations Refs 44 and 45); For in-plane vibrations: C–C stretching vibrations (8a, 8b, 14, 19a, 19b), C–H/X bending vibrations (3, 18a, 18b), radial skeletal vibrations (1, 6a, 6b, 12) C–H stretching vibrations (2, 20a, 20b, 7a, 7b); For out-of-plane vibrations: C–H/X vibrations (5, 10a, 11, 17a, 17b), skeletal vibrations (4, 16a, 16b). δ – in-plane deformation, t – twisting, r – rocking, ω – wagging, sciss. – scissoring, γ – out-of-plane deformation, Δ – in-plane deformation of skeleton atoms, Γ – out-of-plane deformation of skeleton atoms, ip – in phase vibrations, op – out of phase vibrations. Subscripts: carbox – carboxylic. § For MG. † for IPG. $^{\xi}$ for GF. $^{\Psi}$ for DG. * For gallates. ** For gallic acid.

DOI: 10.1002/jrs

interactions must be considered. Furthermore, for most of the ferulates and some of the gallates (e.g. IPG) the ν_{OH} signals are indistinguishable, since they occur as a unique and very broad Raman band, sometimes even overlapped by the intense ν_{CH} features as a result of the large shift due to the intermolecular (O)H···O(=C) and (O)H···O(H) close contacts occurring in the solid.

4. Comparison of the short and long chain esters (e.g. MC *vs* OC, MF *vs* PF, or MG *vs* OG, Fig. 3) clearly evidences the expected increase in the number of ν_{CH} modes (in the 3100 to 2850 cm^{-1} range) as the ester chain elongates. Moreover, the largest elements of the series (OC, OG, DC and DG) display a very similar Raman pattern below 1750 cm^{-1} (Fig. 2). The length of the ester alkyl group was not found to affect the $C_9{=}C_{10}$ stretching mode of the hydroxycinnamates, as could be expected in the light of inductive and mesomeric factors, since these are overruled by the electron delocalisation effect in these highly conjugated systems.
5. For the even-membered caffeates (EC, BC, OC and DC), the combination of the ν_{C-O}/δ_{C-H}, and $\delta_{O-H}/\nu_{C=C\ (ring)}$ modes gives rise to a unique feature between 1300 and 1240 cm^{-1} (which is rather strong for EC, OC and DC, Fig. 2), while for the odd-membered MC and PC it yields a doublet centered at *ca* 1280 cm^{-1}. Indeed, the ethyl, octyl and dodecyl caffeates are easily distinguished from the corresponding gallates through this particular band (a narrow and rather intense feature). IPC deviates from this behaviour, owing to the non-linear nature of its ester chain.
6. For the two esters displaying a branched alkyl chain (IPC and IPG) a simplified vibrational pattern was observed in the 1400–1100 cm^{-1} interval (comprising the δ_{CH} modes), when compared to the corresponding linear propyl esters.

The characteristic $\nu_{C-O_{ester}}$ oscillator ((O=)C–O(R_{ester}) stretching) is detected at about 1180 cm^{-1}, yielding a moderately strong Raman band and a very intense infrared peak (as theoretically predicted,[31] Tables 1, S1 and S3, Figs 2 and S5 (Supplementary Material)). When comparing to the values of the corresponding acid ($\nu_{C-O(H)}$), a high-frequency shift is evident in the esters: e.g. ν_{C-O} = 1210 cm^{-1} for methyl caffeate *vs* ν_{C-O} = 1107 cm^{-1} for caffeic acid; ν_{C-O} = 1185 cm^{-1} for methyl ferulate *vs* ν_{C-O} = 1173 cm^{-1} for ferulic acid. This may be explained by the larger force constant of the C–O bond in the esters relative to the parent carboxylic acid, due to an enhancement of the inductive effect (from the alkyl group) upon esterification.

The 1800–1500 cm^{-1} spectral interval (Fig. 5) deserves special attention. In substituted benzyl derivatives, the aromatic ring is known to yield one or two distinct $\nu_{C=C}$ Raman features with moderate to high intensity, centred around 1600 cm^{-1}.[46,47] In the cinnamates, the side chain C=C stretching band appears at a slightly higher frequency, followed by the $\nu_{C=O}$ mode (from 1740 to 1640 cm^{-1}), often with a very low intensity, sometimes almost undetectable in the Raman spectra. As expected, the gallates display a simpler Raman C=O and C=C stretching pattern when compared to the homologous hydroxycinnamates (except for IPG), since they lack the unsaturated chain C=C bond: the features comprised in this wavenumber range are easily ascribed to two ring $\nu_{C=C}$ modes, the $\nu_{C=O}$ oscillator being detectable only for the methyl, ethyl (very weak band at *ca* 1730 cm^{-1}), isopropyl and butyl systems (Figs 2 and 5(C), Table 1). Nevertheless, for the phenolic systems presently studied this Raman pattern varies considerably (sometimes not straightforwardly), which enables their prompt identification by analysis of the corresponding spectra: e.g. methyl *vs* ethyl and propyl ferulates, or ethyl and isopropyl caffeates *vs* the other elements of the series (Fig. 5(A) and (B)).

Comparison between this data and the corresponding calculated wavenumbers evidences a quite good overall agreement (Tables 1, S1 and S2, Figs S1 and S2 (see Supplementary Material)), although the calculations were performed for the isolated molecule. Actually, the main discrepancies between experimental and theoretical wavenumbers were detected for those vibrational modes that are most affected by intra- and/or intermolecular hydrogen bonds,[46] not considered in the theoretical approach presently used. These close contacts, involving the carbonyl, the ring hydroxyl/methoxy substituents and some of the alkyl ester groups (with O···H distances typically between 180 and 250 pm[18,47]), are responsible for the presence of dimeric entities in the solid phase (Fig. 4) and have been previously reported for analogous hydroxycinnamic esters.[18] Their presence is clearly reflected in the Raman spectra through the shifts of the stretching and deformation modes of the corresponding oscillators (mainly O–H and C=O) to lower and higher wavenumbers, respectively, as compared to the calculated values (for the isolated molecule): $\nu_{OH} - \nu_{exp}$ *ca* 3500 cm^{-1} *vs* ν_{calc} *ca* 3800–3700 cm^{-1}; $\nu_{C=O} - \nu_{exp}$ *ca* 1680–1640 cm^{-1} *vs* ν_{calc} *ca* 1790 cm^{-1}; $\nu_{CO_{ester}} - \nu_{exp}$ *ca* 1180 cm^{-1} *vs* ν_{calc} *ca* 1360–1350 cm^{-1}; $\delta_{O-H} - \nu_{exp}$ *ca* 1450–1100 cm^{-1} *vs* ν_{calc} *ca* 1370–1000 cm^{-1} (Fig. S1 (Supplementary Material)).

Actually, the spectral behaviour presently described – particularly the detection of more than one $\nu_{C=O}$ band *per* sample – reflects the characteristic structural arrangement of this kind of phenolic esters in the solid state, the presence of several distinct dimeric entities (Fig. 4), formed through intermolecular hydrogen bonds such as (C)=O···H(O), (H)O···H_3(C–O)$_{ester}$, (C)=O···H_3(C–O)$_{ring}$ and/or (C)=O···H_3(C–O)$_{ester}$ (previously reported to occur in substituted benzaldehydes,[47] Fig. 4.AIII) or even (C=C)H···O(=C) (proposed to occur in α-substituted cinnamates such as the ones presently studied[48]).

The experimental Raman spectra of the alkyl esters will thus be the sum of the individual pattern of each dimer present in the solid. This hypothesis is corroborated by the Raman data calculated for the isolated molecules

JRS

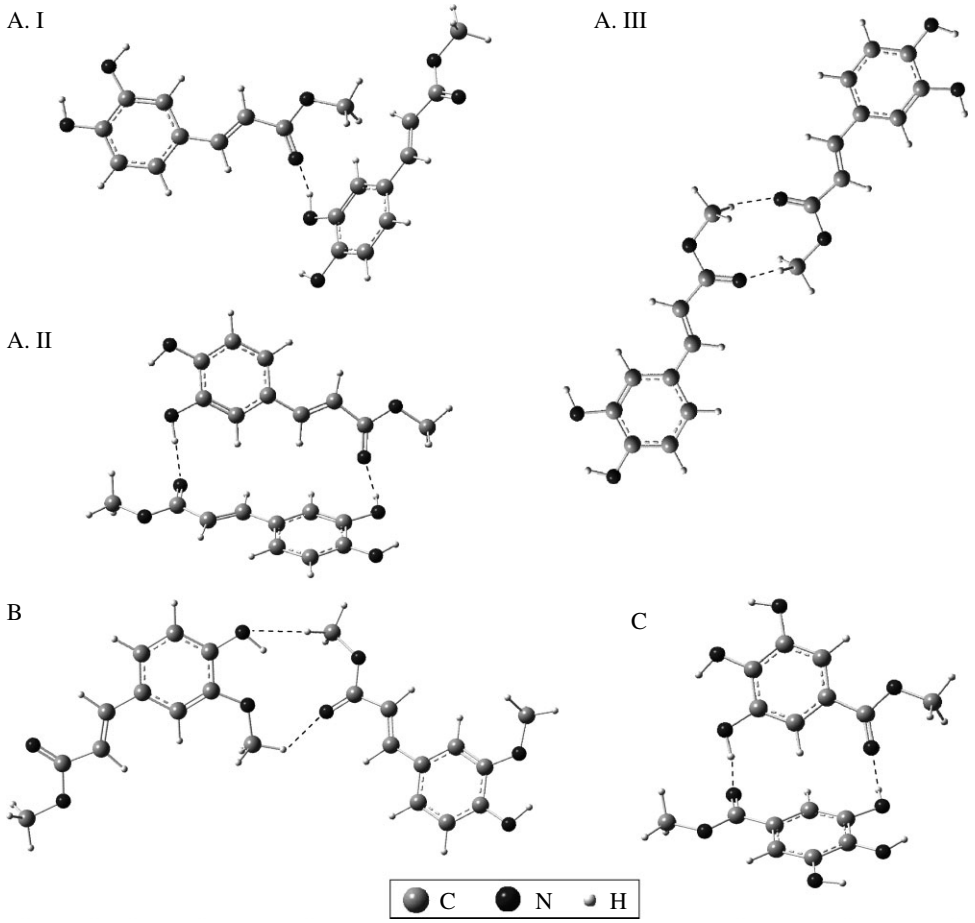

Figure 4. Schematic representation of some dimeric structures proposed for the esters under study. A – methyl caffeate; B – methyl ferulate; C – methyl gallate.

(e.g. MC, Fig. 5(A)), which yield a simpler pattern in the 1800–1500 cm^{-1} region as compared to the experimental one, displaying one intense Raman feature (comprising two overlapped bands) due to the ring $\nu_{C=C}$ modes, one moderately strong signal assigned to the chain $\nu_{C=C}$, and only one $\nu_{C=O}$ band (weak in Raman). In fact, in the light of the dimeric structures proposed for these systems (Fig. 4), $\nu_{C=O}$ is expected to be one of the most affected modes by the monomer–monomer H-bonds, since the (C)=O···H(O) and (C)=O···H_3(C–O)$_{ester}$ are the strongest of these interactions. For the methyl esters, for instance, these close contacts are reflected in the experimental detection of two to three $\nu_{C=O}$ signals, red-shifted (by *ca* 50 cm^{-1}) relative to the only calculated one: $\nu_{C=O}^{exp}$ = 1679 and 1665 cm^{-1} *vs* $\nu_{C=O}^{calc}$ = 1724 cm^{-1}, for MC; $\nu_{C=O}^{exp}$ = 1720, 1702 and 1676 cm^{-1} *vs* $\nu_{C=O}^{calc}$ = 1724 cm^{-1}, for MF; and $\nu_{C=O}^{exp}$ = 1755, 1680 and 1671 cm^{-1} *vs* $\nu_{C=O}^{calc}$ = 1723 cm^{-1} for MG (Fig. 5).

For the ferulates, another possible dimeric geometry has to be taken into account: apart from the dimers formed through (C)=O···H(O) and top-to-top (C)=O···H_3(C–O)$_{ester}$ bonds (as in the caffeates, Fig. 4(A)), (C)=O···H_3(C–O)$_{ring}$ interactions may also occur (Fig. 4(B)). This is reflected in the complex Raman pattern observed for methyl ferulate (Fig. 5(B)) which differs significantly from the much simpler corresponding calculated spectrum. The gallates, in turn, display a lower number of bands in the 1800–1500 cm^{-1} region (Fig. 5(C)), since the side chain C=C bond is absent and the top-to-top dimeric species represented in Fig. 4(C) is expected to be favoured over the others (e.g. Figure 4(A).III), as a result of the medium to strong (C)=O···H(O) close contacts.

When the ester alkyl chain increases in length some of the dimeric species represented in Fig. 4 are highly unfavoured (e.g. dimer A.III), owing to the steric hindrance between those bulkier groups. This is probably the case for the non-linear ester IPC that displays only two intense bands between 1800 and 1500 cm^{-1}, as opposed to the four features clearly detected for its linear analogue PC (Fig. 5(A)).

Furthermore, it should be noted that the $\nu_{C=O}$ wavenumber is largely determined by an equilibrium between inductive and mesomeric effects within these phenolic systems. For the hydroxycinnamates (caffeates and ferulates), the presence of the C_9=C_{10} double bond in the

DOI: 10.1002/jrs

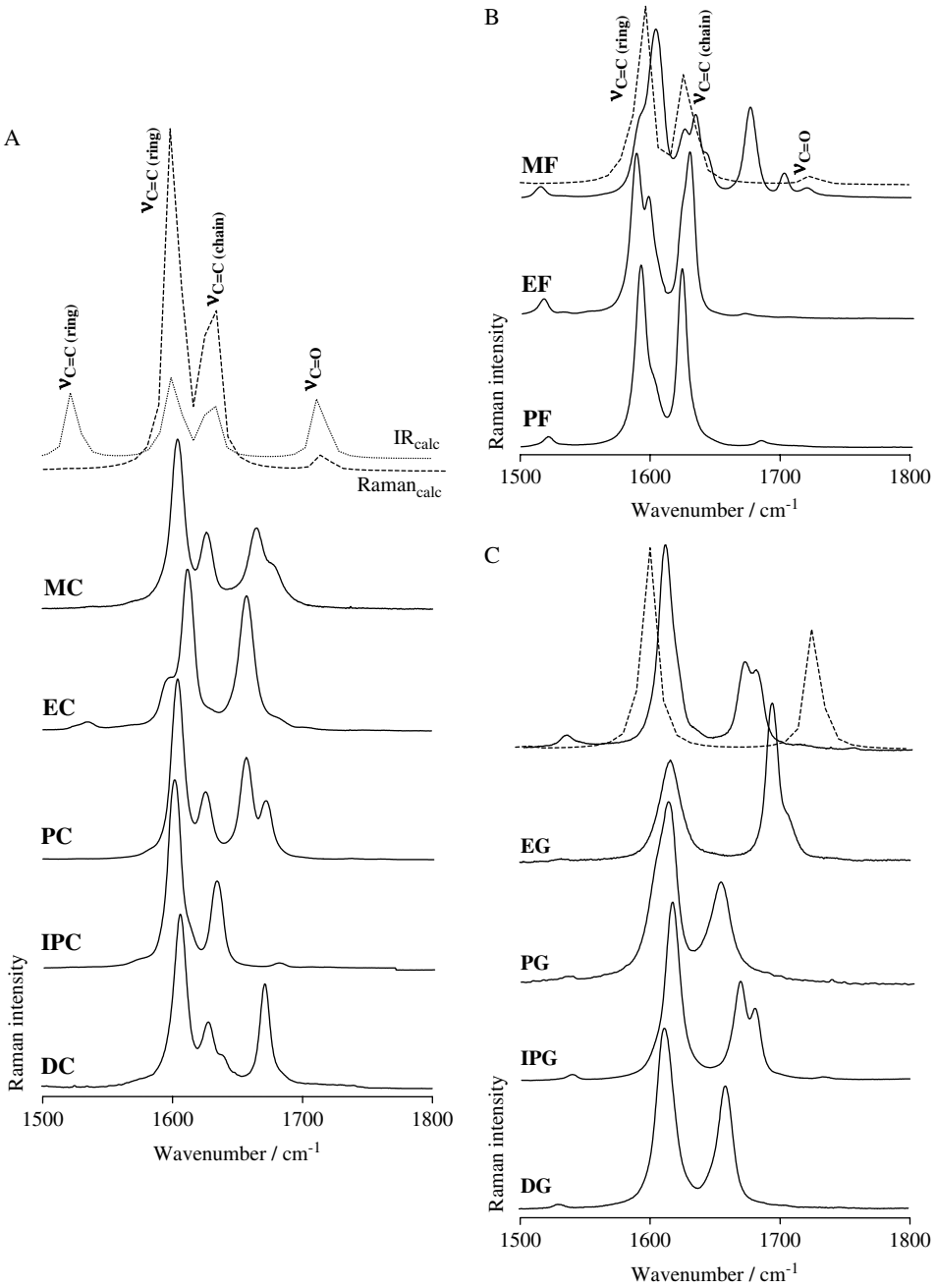

Figure 5. Experimental (solid state, 25 °C) Raman spectra, in the 1500–1800 cm^{-1} region, for some of the phenolic esters studied in the present work. A – caffeates; B – ferulates; C – gallates. The calculated patterns (B3LYP/6-31G**, dotted line) for methyl caffeate, methyl ferulate and methyl gallate are also represented.

bridging chain in conjugation with the ester moiety and aromatic ring allows an extensive conjugation effect – positive mesomerism (+M) – between the whole π-system (ring → C_9═C_{10} → C═O). This is balanced by the negative inductive (−I) and positive mesomeric (+M) effects applied by the aromatic ring on the rest of the molecule. The presence of the methoxy ring substituent in the ferulates is reflected in a different inductive/mesomeric balance, owing to the +I/+M contributions of the methyl group. In the gallates the positive mesomeric influence of the ring is expected to be stronger, thanks to the direct bond of the ester group. Also, the ester alkyl chain is responsible for a positive inductive factor (+I) that increases with the chain length. The latter is responsible for the slight increase of the carbonyl stretching wavenumber when going from a methyl to a dodecyl ester, since the enhancement of the induction due to the ester alkyl group leads to a strengthening of the C═O bond, this effect being more pronounced for the gallates, since the

DOI: 10.1002/jrs

α, β-unsaturation effect is not present in benzoic systems – e.g. $\nu_{C=O}$ varies from 1680 to 1682 and 1704 cm^{-1} for methyl, butyl and octyl gallates, respectively (Tables 1, S1 and S2). As pointed out above, for the hydroxycinnamates (caffeates and ferulates) the π-conjugation overcomes this effect, which is not clearly reflected in the corresponding experimental vibrational wavenumbers.

CONCLUSIONS

A series of antioxidant, variable-length alkyl esters – caffeates, ferulates and gallates – were studied as to their conformational characteristics by Raman spectroscopy. Their solid-state vibrational pattern was assigned in the light of the DFT calculations presently performed for ferulates and gallates, and of previously reported quantum mechanical data for the caffeates.[23,29,31] A good agreement was found between the calculated and experimental wavenumbers, as well as with published results (both theoretical and spectroscopic) on similar molecules, such as CA,[29] the analogous 3,4,5-trihydroxycinnamic acid[29,30] and its ethyl ester,[18] and GA.[49–51] Moreover, unequivocal spectroscopic evidence of the presence of intermolecular H-bonds between the C=O and ring OH/OCH_3 groups of adjacent ester molecules, responsible for the occurrence of dimeric species in the solid, was obtained.

The present study clearly evidences the utility of Raman spectroscopy as a high-sensitivity and non-invasive technique for identifying chemically similar compounds such as these structurally related phenolic esters. Actually, the Raman data presently gathered for this type of phenolic antioxidants yielded particular vibrational features, which enable their ready identification and differentiation based on structural characteristics such as the length and saturation degree of the ester side chain, or the number and nature of the ring substituents. In fact, in the last few years, Raman spectroscopy has proved to be a simple and reliable method for determining the composition profile of solid samples, since it yields unique fingerprint spectra for each compound, and is thus becoming an important tool in forensic and pharmaceutical laboratories, among others (e.g. characterisation of illegal drugs of abuse and their precursors,[52–55] food analysis and study of lead molecules for drug design).

In conclusion, this type of conformational analysis of phenolic derivatives by vibrational spectroscopy coupled to theoretical studies yields reliable structural information, which is essential for the elucidation of the SARs ruling the biological activity of these compounds, mainly when it is combined to biochemical activity evaluation experiments (e.g. antioxidant capacity and cytotoxicity against human cancer cell lines[11,22,23,25,56]). Indeed, this biochemical role and the way it may be modulated by a careful structural design (from a lead compound) can be accurately understood only in the light of a thorough knowledge of the conformational preferences of the systems involved.

Supplementary material

Supplementary electronic material for this paper is available in Wiley InterScience at: http://www.interscience.wiley.com/jpages//suppmat/

Acknowledgements

The authors thank financial support from the Portuguese Foundation for Science and Technology – Project POCI/QUI/55631/2004 (co-financed by the European Community fund FEDER) and PhD fellowships SFRH/BD/16520/2004 and SFRH/BD/17493/2004. The Chemistry Department of the University of Aveiro, where the FT-Raman experiments were carried out, is also acknowledged.

REFERENCES

1. Natella F, Nardini M, Di Felice M, Scaccini C. *J. Agric. Food Chem.* 1999; **47**: 1453.
2. Mattila P, Hellstrom J, Torronen R. *J.Agric.Food Chem.* 2006; **54**: 7193.
3. Lin J-Y, Tang C-Y. *Food Chem.* 2007; **101**: 140.
4. Podsdek A. *Food Sci. Technol.* 2007; **40**: 1.
5. Teixeira S, Siquet C, Alves C, Boal I, Marques MPM, Borges F, Lima JLFC, Reis S. *Free Radic. Biol. Med.* 2005; **39**: 1099.
6. Lee Y-T, Don M-J, Liao C-H, Chiou H-W, Chen C-F, Ho L-K. *Clin. Chim. Acta* 2005; **352**: 135.
7. Suzuki A, Yamamoto N, Jokura H, Yamamoto M, Fujii A, Tokimitsu I, Saito I. *J. Hypertens.* 2006; **6**: 1065.
8. Khanduja KL, Avti PK, Kumar S, Mittal N, Sohi KK, Pathak CM. *Biochim. Biophys. Acta* 2006; **283**: 1760.
9. Siquet C, Paiva-Martins F, Milhazes N, Lima JLFC, Reis S, Borges F. *Free Radic. Res.* 2006; **40**: 433.
10. Cárdenas M, Marder M, Blank VC, Roguin LP. *Bioorg. Med. Chem.* 2006; **14**: 2966.
11. Fresco P, Borges F, Diniz C, Marques MPM. *Med. Res. Rev.* 2006; **26**: 747.
12. Ferguson PJ, Kurowska E, Feeman DJ, Chambers AF, Koropatnick DJ. *J. Nutr.* 2004; **134**: 1529.
13. Wenzel U, Herzog A, Kuntz S, Daniel H. *Proteomics* 2004; **4**: 2160.
14. Yoshimizu N, Otani Y, Saikawa Y, Kubota T, Yoshida M, Furukawa T, Kumai K, Kameyama K, Fujii M, Yano M, Sato T, Ito A, Kitajima M. *Aliment. Pharmacol. Ther.* 2004; **20**: 95.
15. Kintzios S. *Crit. Rev. Plant Sci.* 2006; **25**: 79.
16. Kelloff GJ. *Adv. Cancer Res.* 2000; **78**: 199.
17. Manach C, Scalbert A, Morand C, Rémésy C, Jiménez L. *Am. J. Clin. Nutr.* 2004; **79**: 727.
18. Sousa JB, Calheiros R, Rio V, Borges F, Marques MPM. *J. Mol. Struct.* 2006; **783**: 135.
19. Chung WY, Jung YJ, Surh YJ, Lee SS, Park KK. *Mutat. Res.* 2001; **496**: 199.
20. Krasowska A, Stasiuk M, Oswiecimska M, Kozubek A, Bien M, Witek S, Sigler K. *Z. Naturforsch.* 2001; **56**: 878.
21. Silva FAM, Borges F, Ferreira M. *J. Agric. Food Chem.* 2001; **49**: 3936.
22. Gomes CA, Girãda Cruz T, Andrade JL, Milhazes N, Borges F, Marques MPM. *J. Med. Chem.* 2003; **46**: 5395.
23. Fiuza SM, Van Besien E, Milhazes N, Borges F, Marques MPM. *Bioorg. Med. Chem.* 2004; **12**: 3581.
24. Chung TW, Moon SK, Chang YC, Ko JH, Lee YC, Ch G, Kim JG, Kim CH. *FASEB J.* 2004; **18**: 1670.
25. Marques MPM, Borges F, Sousa JB, Calheiros R, Garrido J, Gaspar A, Antunes F, Diniz C, Fresco P. *Lett. Drug Des. Discov.* 2006; **3**: 316.

26. Graf E. *Free Radic. Biol. Med.* 1992; **13**: 435.
27. Mathew S, Abraham TE. *Crit. Rev. Biotechnol.* 2004; **24**: 59.
28. Wang BH, Ou-Yang JP. *Cardiovasc. Drug Rev.* 2005; **23**: 161.
29. Van Besien E, Marques MPM. *THEOCHEM* 2003; **625**: 265.
30. Fiuza SM, Van Besien E, Milhazes N, Borges F, Marques MPM. *J. Mol. Struct.* 2004; **693**: 103.
31. Machado NFL, Calheiros R, Fiuza SM, Borges F, Gaspar A, Garrido J, Marques MPM. *J. Mol. Model.* 2007; **13**: 865.
32. Borges MFM, Pinto MMM. *J. Liq. Chromatogr.* 1994; **17**: 1125.
33. Silva FAM, Borges F, Guimarães C, Lima JLFC, Matos C, Reis S. *J. Agric. Food Chem.* 2000; **48**: 2122.
34. Frisch MJ, Trucks GW, Schlegel HB, Scuseria GE, Robb MA, Cheeseman JR, Montgomery JA Jr., Vreven T, Kudin KN, Burant JC, Millam JM, Iyengar SS, Tomasi J, Barone V, Mennucci B, Cossi M, Scalmani G, Rega N, Petersson GA, Nakatsuji H, Hada M, Ehara M, Toyota K, Fukuda R, Hasegawa J, Ishida M, Nakajima T, Honda Y, Kitao O, Nakai H, Klene M, Li X, Knox JE, Hratchian HP, Cross JB, Adamo C, Jaramillo J, Gomperts R, Stratmann RE, Yazyev O, Austin AJ, Cammi R, Pomelli C, Ochterski JW, Ayala PY, Morokuma K, Voth GA, Salvador P, Dannenberg JJ, Zakrzewski VG, Dapprich S, Daniels AD, Strain MC, Farkas O, Malick DK, Rabuck AD, Raghavachari K, Foresman JB, Ortiz JV, Cui Q, Baboul AG, Clifford S, Cioslowski J, Stefanov BB, Liu G, Liashenko A, Piskorz P, Komaromi I, Martin RL, Fox DJ, Keith T, Al-Laham MA, Peng CY, Nanayakkara A, Challacombe M, Gill PMW, Johnson B, Chen W, Wong MW, Gonzalez C, Pople JA. *Gaussian 03, Revision B. 04*. Gaussian: Pittsburgh, 2003.
35. Lee C, Yang W, Parr RG. *Phys. Rev.* 1988; **B37**: 785.
36. Miehlich B, Savin A, Stoll H, Preuss H. *Chem. Phys. Lett.* 1989; **157**: 200.
37. Becke AJ. *Phys. Rev.* 1988; **A38**: 3098.
38. Becke AJ. *J. Chem. Phys.* 1993; **98**: 5648.
39. Petersson GA, Bennett A, Tensfeldt TG, Al-Laham MA, Shirley WA, Mantzaris J. *J. Chem. Phys.* 1988; **89**: 2193.
40. Peng C, Ayala PY, Schlegel HB, Frisch MJ. *J. Comput. Chem.* 1996; **17**: 49.
41. Scott AP, Radom L. *J. Phys. Chem.* 1996; **100**: 16502.
42. Batista de Carvalho LAE, Marques MPM, Teixeira-Dias JJC. *J. Chem. Soc., Perkin Trans.* 1999; **2**: 2507.
43. Vueba ML, Pina ME, Veiga F, Sousa JJ, Batista de Carvalho LAE. *Int. J. Pharm.* 2006; **307**: 56.
44. Wilson EB Jr. *Phys. Rev.* 1934; **45**: 706.
45. Varsányi G. *Assignments for Vibrational Spectra of Seven Hundred Benzene Derivates*. Akdémiai Kiadó, Budapest/Adam Hilger Limited: London, 1974.
46. Steiner T. *Angew. Chem. Int. Ed.* 2002; **41**: 48.
47. Ribeiro-Claro PJA, Batista de Carvalho LAE, Amado AM. *J. Raman Spectrosc.* 1997; **28**: 867.
48. Kiss JT, Felfoldi K, Kortvelyesi T, Palinko L. *Vib. Spectrosc.* 2000; **22**: 63.
49. Sánchez-Cortés S, García-Ramos JV. *Spectrochim. Acta* 1999; **A55**: 2935.
50. Sánchez-Cortés S, García-Ramos JV. *Appl. Spectrosc.* 2000; **54**: 230.
51. Sánchez-Cortés S, García-Ramos JV. *J. Colloid Interface Sci.* 2000; **231**: 98.
52. Bell EJ, Burns DT, Dennis AC, Matchett LJ, Speers JS. *The Analyst* 2000; **125**: 1811.
53. Sägmüller B, Schwarze B, Brehm G, Schneider S. *The Analyst* 2001; **126**: 2066.
54. Faulds K, Smith WE, Graham D, Lacey RJ. *The Analyst* 2002; **127**: 282.
55. Milhazes N, Borges F, Calheiros R, Marques MPM. *The Analyst* 2004; **129**: 1106.
56. Milhazes N, Calheiros R, Marques MPM, Garrido J, Natália M, Cordeiro DS, Rodrigues C, Quinteira S, Novais C, Peixe L, Borges F. *Bioorg. Med. Chem.* 2006; **14**: 4078.